Accepted Manuscript

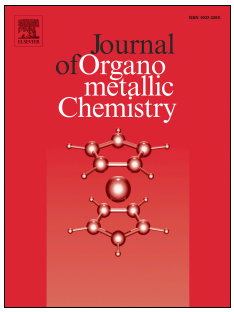

Synthesis, structures and stereodynamic behavior of novel pentacoordinate (O→Si)-Chelate Difluoro(methyl)silylmethyl derivatives of amides and imides

Vadim V. Negrebetsky, Eugeniya P. Kramarova, Aleksander G. Shipov, Yuri I. Baukov, Alexander A. Korlyukov, Dmitry E. Arkhipov, Alan R. Bassindale, Peter G. Taylor, Sergey Yu Bylikin

PII: S0022-328X(18)30297-3

DOI: 10.1016/j.jorganchem.2018.07.027

Reference: JOM 20514

To appear in: *Journal of Organometallic Chemistry*

Received Date: 1 May 2018

Revised Date: 16 July 2018

Accepted Date: 23 July 2018

Please cite this article as: V.V. Negrebetsky, E.P. Kramarova, A.G. Shipov, Y.I. Baukov, A.A. Korlyukov, D.E. Arkhipov, A.R. Bassindale, P.G. Taylor, S.Y. Bylikin, Synthesis, structures and stereodynamic behavior of novel pentacoordinate (O→Si)-Chelate Difluoro(methyl)silylmethyl derivatives of amides and imides, *Journal of Organometallic Chemistry* (2018), doi: 10.1016/j.jorganchem.2018.07.027.

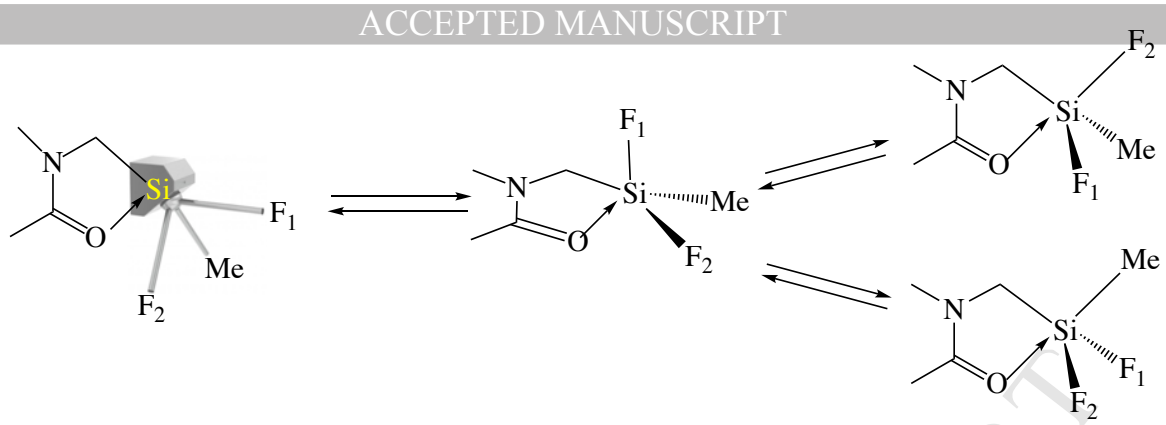

Synthesis, Structures and Stereodynamic Behavior of Novel Pentacoordinate (O→Si)-Chelate Difluoro(methyl)silylmethyl Derivatives of Amides and Imides

Vadim V. Negrebetsky★, Eugeniya P. Kramarova, Aleksander G. Shipov, Yuri I. Baukov

Department of Chemistry, N. I. Pirogov Russian National Research Medical University, Ostrovityanov St. 1, Moscow 117997, Russian Federation; e-mail: negrebetsky1@rsmu.ru

Alexander A. Korlyukov, Dmitry E. Arkhipov

A. N. Nesmeyanov Institute of Organoelement Compounds, RAS, Vavilova St. 28, 11991 Moscow, Russian Federation

Alan R. Bassindale, Peter G. Taylor, Sergey Yu. Bylikin

Department of Chemistry, Open University, Walton Hall, Milton Keynes, MK7 6AA, United Kingdom

ABSTRACT

The structures and stereodynamic behavior of (O→Si)-chelate methyldifluorosilanes in solutions were studied by multinuclear (^{1}H, ^{13}C, ^{19}F, ^{29}Si) and 2D (COSY, HETCOR ^{1}H, ^{13}C) NMR spectroscopy. The range of studied complexes included amides $RC(O)N(R')CH_2SiMeF_2$ [R = Ph, R' = H (**1a**); R = R' = Me (**1b**); R = Me, R' = CHMePh (**1c**)], lactams LCH_2SiMeF_2 (L = 2-oxoazepan-1-yl (**2a**), 2,2-dimethyl-4-oxo-2*H*-benzo[1,3]oxazin-3-yl (**2b**) or 4-methyl-2-oxoquinolin-1-yl (**2c**)] and the six-membered imide Im^6CH_2 [2,6-dioxopiperidin-1-yl (**3**)]. The pentacoordination of silicon atoms in all studied compounds was confirmed by NMR study in solutions and single-crystal X-ray studies of complexes **1c**, **2a**, **2c** and **3**. The temperature dependency observed for ^{19}F NMR signals in solution was explained by the ligand exchange in the coordination environment of silicon atoms (permutational isomerization) and used for determining the activation parameters of this process by ^{19}F DNMR. Quantum-chemical calculations for various isomers of complexes **1c**, **2a**, **2c** and **3** suggested the "turnstile rotation" as the most likely mechanism for the observed stereodynamic processes.

Key words: pentacoordinated difluorosilanes, synthesis, X-ray, dynamic NMR, permutational isomerization, quantum-chemical calculations.

Introduction

Compounds of hypercoordinate silicon continue to attract attention due to their unusual structural features, increased reactivity, biological activity and stereochemical nonrigidity in solution.[1–8] Neutral fluorides of pentacoordinate silicon[9,10] are generally more stable and less susceptible to hydrolysis, so they are commonly used as model compounds in various applications. However, certain

types of these compounds, in particular monochelate difluorosilanes, have not been studied thoroughly.

In the present paper we discuss the synthesis, structures and stereodynamic behaviour in solution of pentacoordinate mono-(O→Si)-chelate (methyldifluorosilyl)methyl derivatives of amides, lactams and imides. The reported compounds were studies by multinuclear (^{1}H, ^{13}C, ^{19}F, ^{29}Si) and 2D (COSY, HETCOR ^{1}H,^{13}C) NMR spectroscopy, quantum-chemical calculations and single-crystal X-ray crystallography.

Results and discussion

Synthesis of pentacoordinate complexes of difluorosilanes

Pentacoordinate mono-(O→Si)-chelate (methyldifluorosilyl)methyl derivatives of amides $RC(O)N(R')CH_2SiMeF_2$ (**1a–c**) were synthesized according to **Scheme 1**. The difluoroderivatives of lactams LCH_2SiMeF_2 (**2a–c**) and imide $Im^6CH_2SiMeF_2$ (**3**) (**Chart 1**) were synthesized by similar procedures. In all cases, the intermediate pentacoordinate methyldichlorosilanes **A** were synthesized either by the reactions of *N*-trimethylsilyl amides, lactams or imides with $ClCH_2Si(Me)Cl_2$ (*a*)[11,12] or by the reactions of respective NH-compounds with a mixture of $(Me_3Si)_2NH$ and $ClCH_2Si(Me)Cl_2$ (*b*)[13,14].

Scheme 1

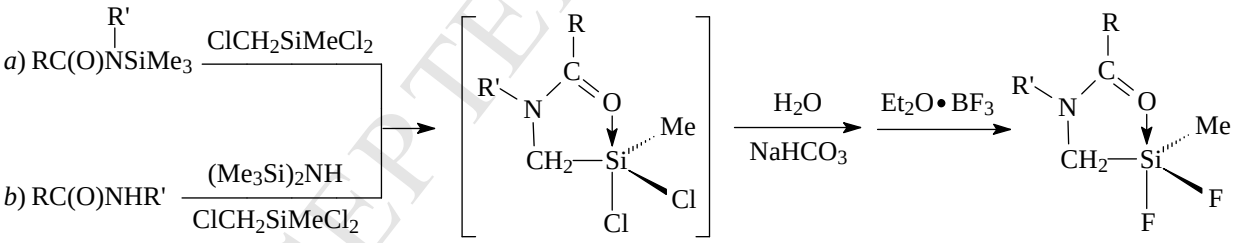

A **1a–c**

R = Ph, R' = H (**1a**); R = R' = Me (**1b**); R = Me, R' = CH(Ph)Me (**1c**)

Chart 1

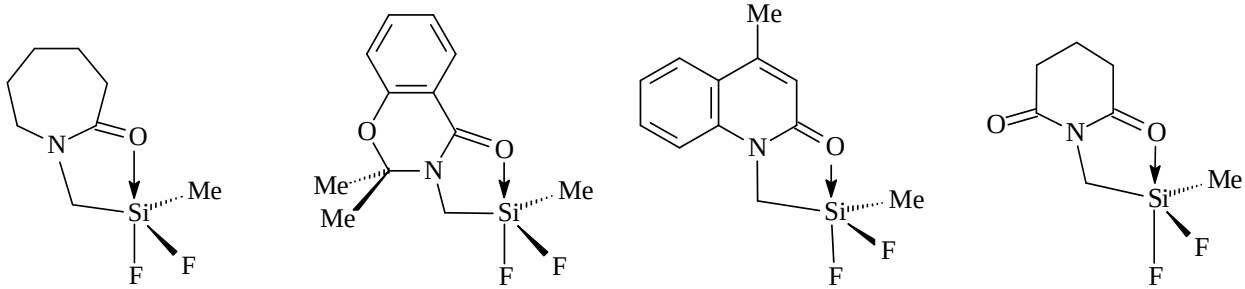

2a **2b** **2c** **3**

Method (*a*) was used for silanes **1a**, **2b**[15], **2c** and **3** while all other silanes were prepared by method (*b*). The hydrolysis of intermediate products **A** was followed by *in situ* reaction of the resulting oligosiloxanes with $BF_3 \cdot Et_2O$, producing target difluorides **1–3** in low to moderate yields (6–68%).

The structures and composition of target compounds was confirmed by elemental analysis, IR and NMR spectroscopy, and single-crystal X-ray diffraction study of complexes **1c**, **2a**, **2c** and **3**. The X-ray structures of difluorides **1b**[16] and **2b**[15] were published earlier.

Single crystal X-ray studies

A single crystal X-ray study of compounds **1c**, **2a, 2c** and **3** confirm that they are difluorosilanes with a five-membered (O→Si)-chelate ring (Figures 1–4).

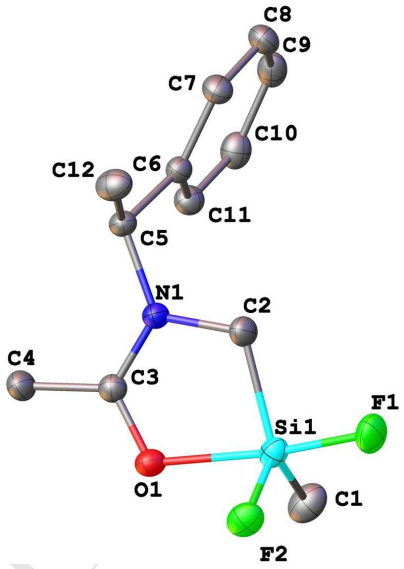

Figure 1. Molecular structure of **1c** in ADP ellipsoids at 50% probability.

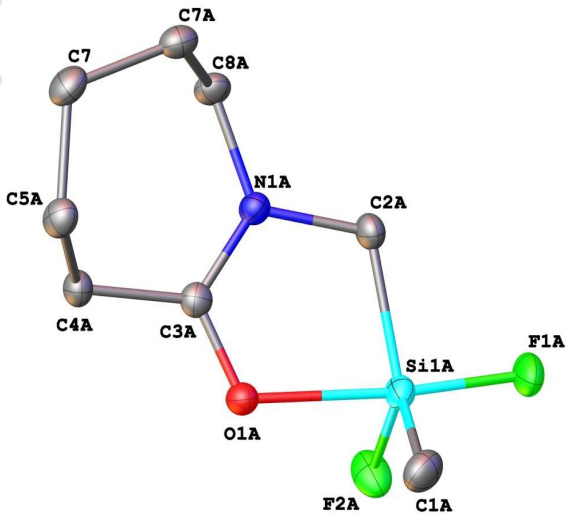

Figure 2. Molecular structure of **2a** in ADP ellipsoids at 50% probability.

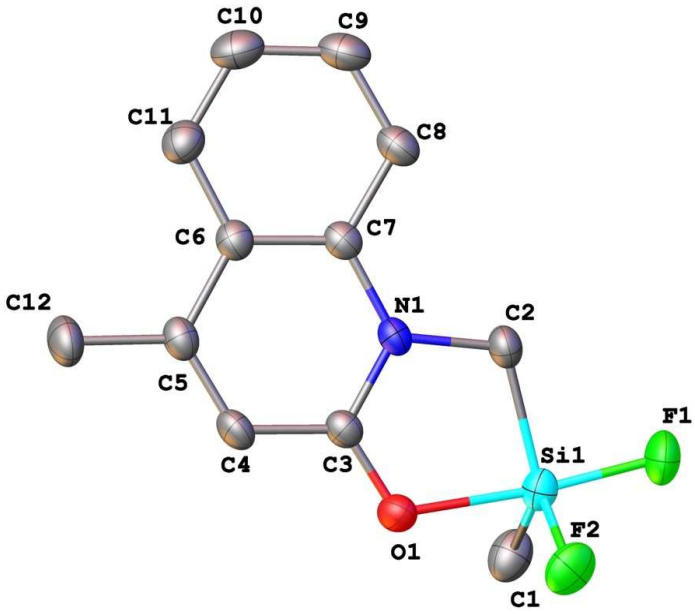

Figure 3. Molecular structure of **2c** in ADP ellipsoids at 50% probability.

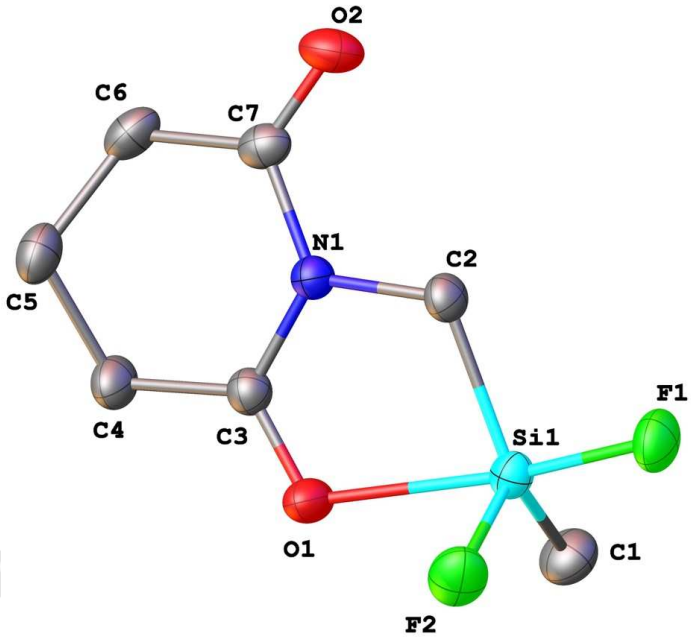

Figure 4. Molecular structure of **3** in ADP ellipsoids at 50% probability.

Only a few crystal structures of similar difluorides have been published to date. Owing to the presence of an equatorial fluorine atom, the Si1–O1 coordination bond in such compounds was expected to be somewhat shorter than that in similar chelates with the Me_2SiF moiety. However, the Si1–O1 distances in (O→Si)-chelate difluorides vary in a wide range from 2.217 Å in methyl(benzoyloxymethyl)difluorosilane[18] to 1.971 Å in *N*-methyl-*N*-(methyldifluorosilylmethyl) acetamide.[16] Thus, the geometry of the MeFOSiF coordination centre is very sensitive to the nature of

the five membered chelate ring and its substituents. The strength of the electron withdrawing effect of the O1 atom depends on substituents at the N1 and C3 positions. Compounds **1c**, **2a**, **2c**, and **3** contain several types of aromatic and alkyl moieties bonded to the N1 and C3 atoms and so the Si1–O1 distances in these difluorosilanes varies in the range of 1.95–2.16 Å (Table 1).

Table 1. Selected bond length (Å) and angles (°) in complexes **1c**, **2a**, **2c** and **3**.

	1c	**2a**	**2c**	**3**
Si1—F1	1.6607(12)	1.6566(13)	1.6571 (11)	1.6380(12)
Si1—F2	1.6094(11)	1.6149(11)	1.6056 (10)	1.5972(12)
Si1—O1	2.0072(13)	2.0004(14)	1.9507 (11)	2.1599(16)
Si1—C1	1.841(2)	1.852(2)	1.8918 (15)	1.831(2)
Si1—C2	1.8844(19)	1.891(2)	1.8428 (16)	1.8769(19)
O1—C3	1.269(2)	1.271(3)	1.2764 (16)	1.2367 (19)
F1–Si1–O1	172.41(6)	173.65(8)	171.48(5)	171.97(5)

The presence of a piperidine-2,6-dione ring in **3** reduces the ability of the O1 atom to donate electrons, which causes the elongation of the Si1–O1 bond to 2.1599(16) Å. In contrast, the aromatic 4-methylquinoline fragment in **2c** increases the electron-donating ability of the O1 atom and, as a consequence, leads to a considerable shortening of the Si1–O1 bond. It should be noted that the Si1–O1 distance in **2c** is even shorter than in *N*-methyl-*N*-(methyldifluorosilylmethyl)acetamide.[16]

The lengths of apical Si1–F1 and equatorial Si1–F2 bonds differ by 0.04–0.05 Å. The longest Si1–F1 bond, 1.6607(12) Å, was found in **1c** while the Si1–F1 distances in **2c** and **2a** were only slightly shorter. The electron-withdrawing effect of the piperidine-2,6-dione ring in **3** caused a more noticeable shortening of the Si1–F1 bond, down to 1.6380(12) Å.

Variable-temperature NMR ^{19}F studies

At ambient temperature, the ^{19}F signals in NMR spectra of difluorosilanes **1** and **2** appear as singlets at –120 to –130 ppm due to a fast (on NMR time scale) positional exchange of the equatorial (F_e) and apical (F_a) fluorine atoms. At temperatures below –40 °C, this exchange slows down significantly, producing two separate $^{19}F_a$ and $^{19}F_e$ signals of equal intensity at approximately –100 and –145 ppm, respectively (Fig. 5). The DNMR spectra of complex **3** are complicated by continuous re-coordination of the silicon atom between the two carbonyl groups.

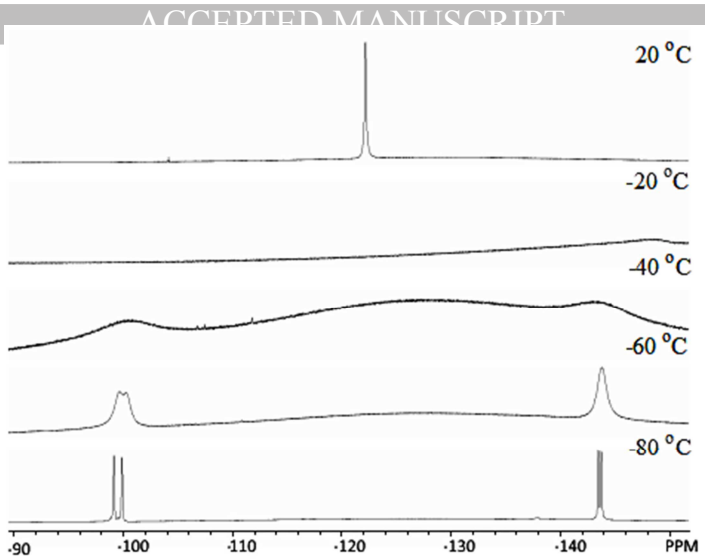

Figure 5. DNMR ^{19}F spectra of difluoride **1c** (Jeol JNM-EX400, CD_2Cl_2 + $CDCl_3$).

The additional splitting of $^{19}F_a$ and $^{19}F_e$ signals observed in low-temperature NMR spectra of difluorides **1c** and **2a** is caused by the presence of chiral carbon centers in their chelate ligands. Below –75 °C, the NMR spectra of these compounds in equimolar mixtures of $CDCl_3$ and CD_2Cl_2 show two pairs of doublets with integral ratios of 1 : 1 ($^2J_{F_a-F_e}$ ~ 23 Hz), which correspond to two diastereomers. In the case of **1c**, these signals appear at $\delta(^{19}F)$ = –99.18, –99.91, –143.48 and –143.75 ppm (Fig. 5).

The activation parameters of the permutational isomerization in difluorides **1** and **2** were calculated[19] from DNMR ^{19}F data (Table 2).

Table 2. Activation parameters of the permutational isomerization of difluorides $RC(O)N(R')CH_2SiMeF_2$ (**1a**–**c**) and LCH_2SiMeF_2 (**2a**–**c**) in $CDCl_3$ + CD_2Cl_2.

Compound	$\Delta G^{\#}_{298}$, kcal mol^{-1}	$\Delta H^{\#}$, kcal mol^{-1}	$\Delta S^{\#}$, cal mol^{-1} K^{-1}	T, K
1a	9.6 ± 0.2	11.3 ± 0.2	7 ± 2	245
1b	9.7 ± 0.3	11.1 ± 0.1	6 ± 3	234
1c	9.6 ± 0.2	10.8 ± 0.2	4 ± 3	239
2a	9.7 ± 0.2	11.2 ± 0.2	7 ± 2	241
2b	9.9 ± 0.2	13.3 ± 0.2	14 ± 3	244
2c	9.7 ± 0.2	10.9 ± 0.2	5 ± 2	240

The positional exchange of fluorine atoms in difluorides **1** and **2** is characterized by a relatively low activation barrier (9.6–9.9 kcal mol^{-1}) and a positive entropy of activation (4–14 cal mol^{-1} K^{-1}, Table 2). These parameters differ significantly from the $\Delta G^{\#}_{298}$ and $\Delta S^{\#}$ values observed for monofluorides $LCH_2SiMe(R)F$ (R = Me, Ph) (ca. 24 kcal mol^{-1} and –20 cal mol^{-1} K^{-1}, respectively)[10,20], which suggests that stereodynamic processes in these complexes proceed via different mechanisms. Within the studied concentration range (0.02–0.30 M), the activation parameters for difluorides remain virtually unchanged, which is typical for intramolecular processes.

Earlier we found that the permutational isomerization in (O→Si)-chelate monofluorides of pentacoordinate silicon involved an "open" intermediate produced via reversible cleavage of the O→Si coordination bond.[9,10] According to X-ray data, the O→Si distance in the difluoride $MeC(O)N(CHMePh)CH_2SiMeF_2$ (**1c**) is 2.007 Å, which is significantly shorter than that in the structurally similar monofluoride $MeC(O)N(CHMePh)CH_2SiMe_2F$ (2.149 Å).[21] The cleavage of this bond in **1c** would have an activation barrier of over 24 kcal mol^{-1}, which contradicts the experimental data (Table 2). Therefore, the positional exchange of fluoride ligands in difluorides **1** and **2** is unlikely to involve the cleavage of the O→Si coordination.

Quantum chemical calculations of permutational isomerization in difluorides

The available X-ray and DNMR data are insufficient for elucidating the exact pathway of the permutational isomerization in complexes **1** and **2**. Additional information can be obtained from quantum-chemical calculations that allow the characterization of all possible stationary points (supporting materials, Table 1s) on the potential energy surface (PES) and then the determination of the lowest energy pathways between these points.

The stationary points on the PES of **1c**, **2a**, **2c** and **3** include the structures with intramolecular O→Si bonds (*c*), acyclic forms without such bonds (*a*) and the structures where methyl groups are in an apical position (*mea*). Our calculations suggest that the molecular geometries of the complexes with intramolecular O→Si bonds in $CDCl_3$ are very similar to those in crystal. The acyclic forms of all studied complexes are less stable, as the elongation of the O→Si bond increases the total energy by 4–11 kcal mol^{-1}, both in the gas phase and in $CDCl_3$ solution (Fig. 6).

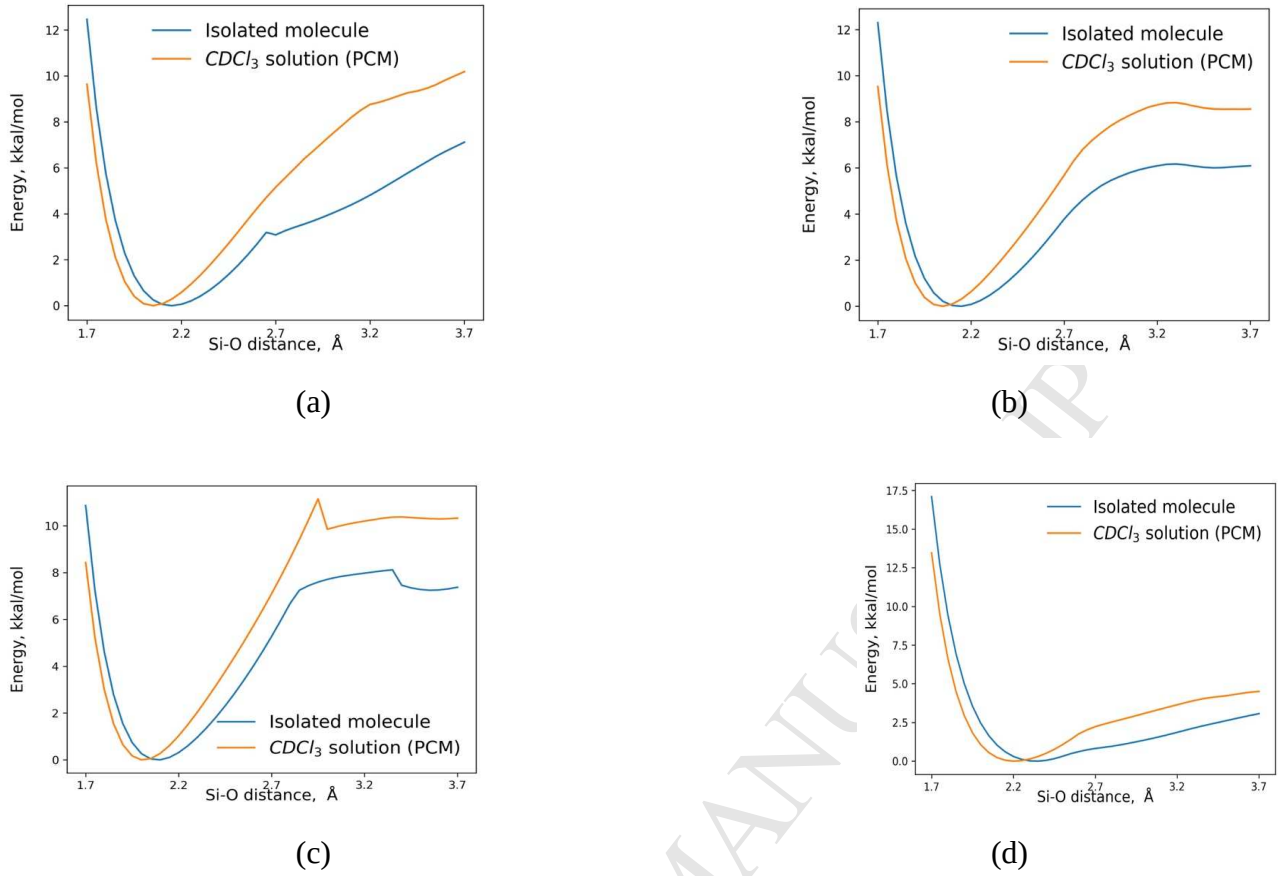

Figure 6. Relaxed energy scan using the O→Si coordination bond as the coordinate for **1c** (a), **2a** (b), **2c** (c), and **3** (d).

The acyclic form of **1c** could be detected neither in the gas phase nor in solution. In contrast, the acyclic forms of other complexes could exist in $CDCl_3$ but not in isolated molecules. In all cases, the structures with the O→Si coordination and the equatorial methyl group were the most stable while the acyclic forms were up to 11 kcal mol^{-1} less favorable (Fig. 7).

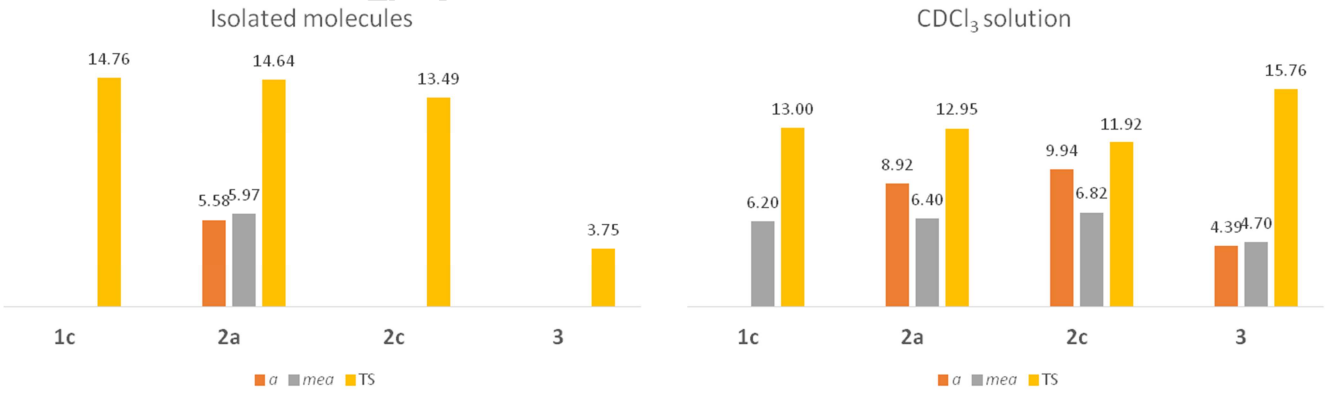

Figure 7. The energies (kcal mol^{-1}) of stationary points and transition states found on the PES of molecules **1c**, **2a**, **2c** and **3** in the gas phase (left) and in $CDCl_3$ solution (right). All values are relative to the most stable cyclic isomer.

In $CDCl_3$, the acyclic forms of **2a** and **2c** are even less stable than the structures with apical methyl groups. According to our calculations, the formation of *mea* structures is not possible without the cleavage of the O→Si coordination bond. The most obvious way to produce a *mea* structure would involve the formation of an acyclic form with subsequent rotation around the Si1–C2 bond.

The search for transition states (TS) produced structures that were intermediate between square pyramid and trigonal bipyramid. The only exception was isolated molecule **3**, where the TS was on the pathway between O1→Si1 and O2→Si1 coordination and had a rather low potential barrier of 3.8 kcal mol^{-1}. However, the use of the PCM model led to a different structure that resembled the TS of other compounds. In both isolated molecules and $CDCl_3$ solutions, the imaginary frequencies of all TS were between 30 and 70 cm^{-1}. The potential barriers determined by the IRC model for the interconversion between TS and the structures with O→Si coordination were in the range 11.9–15.8 kcal mol^{-1}, which is close to the barriers for structurally similar trifluorides (10.2–10.8 kcal mol^{-1})**[17]** and the experimental $\Delta G^{\#}_{298}$ values for complexes **1** and **2** (9.6–9.9 kcal mol^{-1}, Table 2). Therefore, the permutational isomerization in complexes **1** and **2** probably proceeds in a fashion similarly to a turnstile rotation**[22,23]** and involves the positional exchange of fluorine atoms with the retention of the O→Si coordination (Scheme 2).

Scheme 2

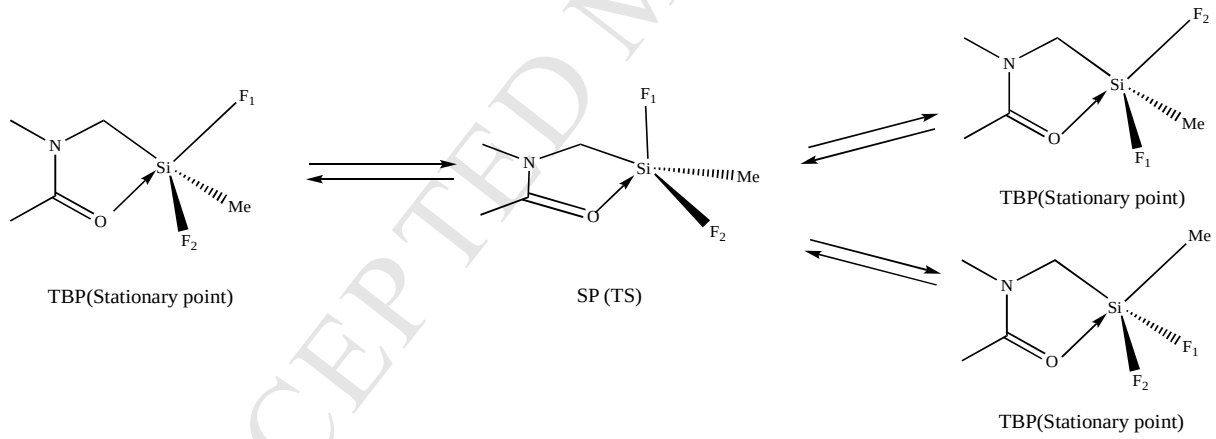

Conclusions

New mono-(O→Si)-chelate methyldifluorosilyl derivatives of amides (**1**), lactams (**2**) and imide (**3**) were synthesized and studied by NMR, IR and X-ray methods. All complexes contain a pentacoordinate silicon atom with one apical and one equatorial fluorine atoms (F_a and F_e, respectively). According to X-ray data, the Si–F_a distances in compounds **1c**, **2a, 2c** and **3** are 0.04–0.05 Å longer than the Si–F_e distances.

The temperature dependency observed for NMR ^{19}F signals of complexes **1** and **2** in solutions is a result of a permutational isomerization in the coordination environment of silicon. Quantum

chemical calculations suggest that the most likely mechanism of this isomerization is the positional exchange of F_a and F_e atoms with the retention of the O→Si coordination, which is similar to the turnstile rotation mechanism.

Experimental section

IR spectra of compounds in solution and in the solid state were recorded on a Bruker Tensor-27 spectrometer using KBr cells and an APR element, respectively. ^{1}H, ^{13}C and ^{19}F NMR spectra in $CDCl_3$ were recorded on a Bruker Avance II 300 (^{1}H, 300 MHz; ^{13}C, 75.6 MHz; ^{19}F, 282.2 MHz) and Jeol JNM-EX400 (^{1}H, 400 MHz; ^{13}C, 100.6 MHz; ^{19}F, 376.3 MHz) instruments using standard pulse sequences.

The ^{1}H, ^{13}C, ^{29}Si chemical shifts were measured using Me_4Si as external reference. Negative values are to high field.

The temperature calibration of the NMR spectrometers was performed by measuring the differences in chemical shifts between non-equivalent protons in methanol (–90…+30 °C) and ethyleneglycol (+30…+85 °C).[24]

The activation parameters of the permutational isomerization were calculated using DNMR-SIM software[25] and a modified Eyring equation[19]. In each case, at least twelve temperature points were obtained to achieve a correlation coefficient of 0.997–0.999.

Single crystals suitable for X-ray diffraction analysis were obtained from the following solvents or mixtures: octane–benzene, 5:2 (**1c**); octane–benzene, 2:1 (**2a**); benzene (**2c**); hexane (**3**). The details of crystallographic data and experimental conditions are given in Table 3.

Table 3. Crystallographic data for compounds **1c**, **2a**, **2c**, and **3**.

	1c	**2a**	**2c**	**3**
Brutto formula	$C_{12}H_{17}F_2NOSi$	$C_8H_{15}F_2NOSi$	$C_{12}H_{13}F_2NOSi$	$C_7H_{11}F_2NO_2Si$
Formula weight	257.35	207.30	253.32	207.26
T, K	120	120	200	173
Diffractometer	Bruker APEX II	Bruker APEX II	Syntex $P2_1$	Bruker Smart 1000
Space group	$P2_12_12_1$	$Pca2_1$	P–1	$P2_1/c$
Z	4	4	2	4
a, Å	10.3448(4)	8.9150(6)	5.2373(17)	12.704(9)
b, Å	10.9723(5)	18.4947(12)	8.867(3)	7.435(4)
c, Å	11.3822(5)	12.1393(8)	12.867(4)	9.793(6)
α, °	90	90	80.33(3)	90.00
β, °	90	90	86.07(3)	92.68(5)
γ, °	90	90	82.73(3)	90.00
V, $Å^3$	1291.95(10)	2001.5(2)	583.6(3)	923.9(10)
d_{calc}, g cm^{-3}	1.323	1.376	1.442	1.490
μ, cm^{-1}	1.90	2.26	2.09	2.53
F(000)	544	880	264	432
$2\theta_{max}$, °	63.48	60.66	50	54
Reflections collected	18645	22206	3093	2135
Independent reflections	4381	6170	2798	2014
Independent reflections [$I > 2\sigma(I)$]	4020	6380	2321	1828
Parameters	157	237	156	119
R_1 [$I > 2\sigma(I)$]	0.0336	0.0318	0.0361	0.0335
wR_2	0.0882	0.0801	0.1126	0.0988
GOF	1.029	1.028	1.064	1.064
Residual electron density, $e \cdot Å^{-3}$(ρ_{min}/ρ_{max})	0.332/–0.273	0.279/–0.202	0.437/–0.288	0.447/–0.289

The structures were solved by the direct method using XS software[26] and refined using a full-matrix least-squares technique against F^2 in the anisotropic-isotropic approximation using SHELXL software.[27] The hydrogen atoms were placed in geometrically calculated positions and refined using a rigid body model [U_{iso}(H) = 1.2U_{eq}(CH, CH_2), U_{iso}(H) = 1.5U_{eq}(CH_3)]. Preparation of graphic materials was performed using OLEX2 software.[28] Crystallographic data for the structural analysis of **1c**, **2a**, **2c** and **3** have been deposited with the Cambridge Crystallographic Data Centre (CCDC Nos.

1834453 – 1834456).

Quantum-chemical calculations of **1c**, **2a**, **2c** and **3** were carried out using Gaussian 03W software. [29]

Hybrid PBE0 functional and 6-311G(d,p) basis sets were used for structure optimization, hessian calculations, relaxed potential energy scans and transition state search. To account for the effect of nonspecific solvation, the PCM model was applied (using the value of the dielectric constant for chloroform). All calculations were carried out with tight optimization criteria (Opt=tight) and precise grid for computation of two-electron integrals (Int(Grid=Ultrafine)). Molecular plots was drawn with ChemCraft software. [30]

Optical rotations of compounds were measured in 10 cm cuvettes using a Perkin Elmer 341 instrument.

The starting materials (hexamethyldisilazane, dichloro(chloromethyl)(methyl)silane, boron trifluoride–diethyl ether complex and 4-methylquinolin-2-one) and solvents were obtained from *Acros* and *Sigma-Aldrich*. The synthesis of (O→Si)-chelate 1-(methyldifluorosilylmethyl)hexahydroazepin-2-one (**2a**)[13] and the X-ray structures of difluorides **1b**[16] and **2b**[15] were published earlier.

6.1. N-Trimethylsilyl (TMS) derivatives

N-TMS-amides and *N*-TMS-glutarimide were prepared by the reactions of respective NH-compounds with chlorotrimethylsilane in the presence of triethylamine or hexamethyldisilazane.[31]

6.1.1. N-TMS-benzamide

Yield 67%, m. p. 103–106 °C (benzene).[31]

6.1.2. 4-Methyl-N-TMS-quinolin-2-one

Yield 91%, b. p. 152–153 °C (10 mm Hg). Found, %: C 67.60, H 7.40, N 5.89. $C_{13}H_{17}NOSi$. Calculated, %: C 67.49, H 7.41, N 6.05. IR spectrum ($CHCl_3$, ν, cm^{-1}): 1670 s, 1615 s, 1510 m (C=O). NMR ^1H spectrum (acetone-d_6, δ, ppm): 0.1 s (9H, $Si(Me)_3$), 2.08 s (3H, CH_3), 6.42 m (H, CH=), 7.0–8.1 m (4H, Ar).

6.1.3. N-TMS-glutarimide

Yield 72%, b. p. 80–82 °C (0.5 mm Hg), n_D^{20} 1.4728. Found, %: C 51.70; H 8.10; Si 15.00. $C_8H_{15}O_2NSi$. Calculated, %: C 51.85; H 8.15; Si 15.15. IR spectrum ($CHCl_3$, ν, cm^{-1}): 1670 s, 1720 s (C=O). NMR ^1H (CCl_4, δ, ppm): 0.28 s (Me), 1.85 m (CCH_2C) 2.42 s (NCH_2). NMR ^{29}Si (CCl_4, δ, ppm): 13.8.

6.2. (O→Si)-chelate N-methyldifluorosilylmethyl amides

*6.2.1. N-(methyldifluorosilylmethyl)benzamide (**1a**)*

A mixture of *N*-TMS-benzamide (5.0 g, 20 mmol) and dichloro(chloromethyl)(methyl)silane (4.24 g, 26 mmol) was heated at 120–140 °C until all chlorotrimethylsilane was distilled off. The remaining mixture was dissolved in 25 mL of chloroform and stirred with a solution of $NaHCO_3$ (4.37 g, 52 mmol) in 50 mL of water for 1 h. The organic layer was separated, the volatiles were removed in vacuum, and the residue was heated with $BF_3 \cdot Et_2O$ (2.46 g, 17 mmol) at 100–120 °C for 30 min. The residue was recrystallized from a mixture of *o*-xylene and octane (3:1) to afford 3.8 g (68%) of difluoride **1a** with m. p. 98–99 °C. Found, %: C 50.18; H 5.16; Si 12.96. $C_9H_{11}F_2NOSi$. Calculated, %: C 50.21; H 5.15; Si 13.05. IR spectrum (neat solid, *ν*, cm^{-1}): 1580 s, 1603 s (NCO). NMR ^1H ($CDCl_3$, *δ*, ppm,): 0.51 br.t (3H, MeSi, $^3J_{HF}$ 5.1 Hz), 2.73 m (2H, NCH_2Si), 7.2 br.s (1H, NH), 7.5–7.9 m (5H, C_6H_5). NMR ^{13}C ($CDCl_3$, *δ*, ppm): 0.42 br.t (MeSi, $^2J_{CF}$ 21.8 Hz), 28.54 t (NCH_2, $^2J_{CF}$ 30.2 Hz), 127.54 s (C^{meta}), 128.61 s (C^{para}), 129.03 s (C^{orto}), 133.51 s (C^{ipso}), 170.45 s (C=O). NMR ^{19}F ($CDCl_3$, *δ*, ppm): –125.40. NMR ^{29}Si ($CDCl_3$, *δ*, ppm): –43.54 t ($^1J_{SiF}$ 256.9 Hz).

*6.2.2. N-(methyldifluorosilylmethyl)-N-methylacetamide (**1b**)*

A solution of *N*-methylacetamide (14.6 g, 0.20 mol), hexamethyldisilazane (12.8 g, 80 mmol) and dichloro(chloromethyl)(methyl)silane (32.6 g, 0.20 mol) in 100 mL of benzene was refluxed for 1 h, then cooled down and stirred with a solution of $NaHCO_3$ (50 g, 0.59 mol) in 200 mL of water overnight. The organic layer was separated, dried over anhydrous $MgSO_4$ and evaporated in vacuum to dryness. The residue was heated with $BF_3 \cdot Et_2O$ (19.8 g, 0.14 mol) at 100–120 °C for 30 min, then distilled in vacuum to afford 9.6 g (29%) of difluoride **1b** with b. p. 135–137 °C (4 mm Hg). Found, %: C 35.96; H 6.60; N 8.26. $C_5H_{11}F_2NOSi$. Calculated, %: C 35.90; H 6.63; N 8.37. IR spectrum ($CHCl_3$, *ν*, cm^{-1}): 1510 s, 1600 s (NCO). NMR ^1H ($CDCl_3$, *δ*, ppm): 0.33 t (3H, MeSi, $^3J_{HF}$ 5.1 Hz), 2.17 s (3H, CMe), 3.11 s (3H, NMe), 2.50 br.s (2H, NCH_2). NMR ^{13}C ($CDCl_3$, *δ*, ppm): 0.34 br.t (MeSi, $^2J_{CF}$ Hz), 17.19 s (CMe), 37.36 s (NMe), 37.97 t (NCH_2, $^2J_{CF}$ 29.2 Hz), 173.27 s (C=O). NMR ^{19}F ($CDCl_3$, *δ*, ppm): –124.12. NMR ^{29}Si ($CDCl_3$, *δ*, pm): –54.71 t ($^1J_{SiF}$ 258.1 Hz).

*6.2.3. N-(methyldifluorosilylmethyl)-N-(1-phenylethyl)acetamide (**1c**)*

A solution of *N*-(1-phenylethyl)acetamide (16.3 g, 0.10 mol) {$[\alpha]_D^{20}$ –124° (*c* 0.019, CH_2Cl_2)}, hexamethyldisilazane (6.4 g, 40 mmol) and dichloro(chloromethyl)(methyl)silane (16.3 g, 0.10 mol) in 50 mL of benzene was refluxed for 1 h, then cooled down and stirred with a solution of $NaHCO_3$ (25 g, 0.29 mol) in 150 mL of water for 1 h. The organic layer was separated, evaporated in vacuum to dryness and heated with $BF_3 \cdot Et_2O$ (9.9 g, 70 mmol) at 100–120 °C for 15 min. The residue was

cooled down and triturated with 50 mL of diethyl ether. The powder formed was recrystallized from 150 mL of benzene to afford 12.4 g (48%) of difluoride **1c** with m. p. 128–130 °C (octane–benzene, 5:2), $[\alpha]_D^{20}$ –26.3° (*c* 0.021, CH_2Cl_2). Found, %: C 55.87; H 6.65. $C_{12}H_{17}F_2NOSi$. Calculated, %: C 56.00; H 6.66. IR spectrum (CH_2Cl_2, *v*, cm^{-1}): 1578 s, 1510 m (NCO). NMR ^1H ($CDCl_3$, *δ*, ppm): 0.34 t (3H, SiMe, $^3J_{HF}$ 5.3 Hz), 1.69 d (3H, *C–CH_3, $^3J_{HH}$ 6.7 Hz), 2.33 s (3H, CH_3CO), 2.14, 2.46 dd (2H, NCH_2, $^2J_{HH}$ 17.2 Hz), 5.09 q (1H, *C–CH, $^3J_{HH}$ 6.7 Hz), 7.2–7.4 m (5H, C_6H_5). NMR ^{13}C ($CDCl_3$, *δ*, ppm): 0.57 t (SiMe, $^2J_{CF}$ 23.3 Hz), 17.68 s ($\underline{C}H_3CH$), 17.79 s ($\underline{C}H_3C(O)$), 28.66 t (NCH_2, $^2J_{CF}$ 30.5 Hz), 56.13 s (CH), 126.37 s (C^{meta}), 128.44 s (C^{para}), 129.18 s (C^{orto}), 138.17 s (C^{ipso}), 172.81 s (C=O). NMR ^{19}F (room temperature, $CDCl_3$, *δ*, ppm): –123.41 br.s. NMR ^{29}Si ($CDCl_3$, *δ*, ppm): –55.47 t ($^1J_{SiF}$ 258 Hz).

*6.2.4. N-(methyldifluorosilylmethyl)-4-methylquinolin-2-one (**2c**)*

Dichloro(chloromethyl)(methyl)silane (4.9 g, 30 mmol) was added dropwise to an ice-cold solution of 4-methyl-*N*-TMS-quinolin-2-one (7.0 g, 30 mmol) in 20 mL of $CHCl_3$. The reaction mixture was stirred overnight, then diluted with 50 mL of $CHCl_3$ and stirred with a solution of $NaHCO_3$ (6.0 g, 70 mmol) in 100 mL of water for 24 h. The organic layer was separated, evaporated in vacuum to dryness and heated with $BF_3 \cdot Et_2O$ (4.26 g, 30 mmol) at 100–120 °C for 30 min. The residue was recrystallised from 100 mL of benzene to afford 3.0 g (39%) of difluoride **2c** with m. p. 187–189 °C (benzene). Found, %: C 56.37, H 5.04, N, 5.39. $C_{12}H_{13}F_2NOSi$. Calculated, %: C 56.99, H 5.17, N 5.53. IR spectrum ($CHCl_3$, *v*, cm^{-1}): 1637 s, 1577 m (NCO). NMR ^1H ($CDCl_3$, *δ*, ppm): 0.46 t (3H, MeSi, $^3J_{HF}$ 5.35 Hz), 2.66 s (3H, Me), 3.24 s (2H, NCH_2Si), 6.86 s (1H, H^3), 7.92 d (1H, H^6, $^3J_{HH}$ 7.9 Hz), 7.79 t (1H, H^7, $^3J_{HH}$ 7.9 Hz), 7.51 t (1H, H^8, $^3J_{HH}$ 7.9 Hz), 7.68 d (1H, H^9, $^3J_{HH}$ 7.9 Hz). NMR ^{13}C ($CDCl_3$, *δ*, ppm): 0.80 t (MeSi, $^2J_{CF}$ 23.9 Hz), 19.58 s (Me), 32.01 t (NCH_2, $^2J_{CF}$ 33.2 Hz), 114.34 s (C^3), 115.42 s (C^9), 122.29 s (C^4), 124.45 s (C^8), 125.77 s (C^7), 132.26 s (C^6), 137.87 s (C^5), 151.96 s (C^{10}), 162.52 s (C=O). NMR ^{19}F (room temperature, $CDCl_3$, *δ*, ppm): –121.65 br.s. NMR ^{29}Si ($CDCl_3$, *δ*, ppm): –58.96 t ($^1J_{SiF}$ 254.3 Hz).

*6.3. N-(methyldifluorosilylmethyl)glutarimide (**3**)*

A mixture of N-TMS-glutarimide (7.4 g, 40 mmol) and dichloro(chloromethyl)(methyl)silane (6.25 g, 40 mmol) was heated at 120–140 °C until all chlorotrimethylsilane was distilled off. The residue was cooled down and stirred with a mixture of 40 mL of chloroform and a solution of $NaHCO_3$ (8.0 g, 0.10 mol) in 60 mL of water for 1 h. The organic layer was separated, evaporated in vacuum to dryness and heated with $BF_3 \cdot Et_2O$ (3.7 g, 26 mmol) at 100–120 °C for 30 min. The residue was recrystallised from 50 mL of hexane to afford 0.5 g (6%) of difluoride **3** with m. p. 73–75 °C (hexane).

Found, %: C 40.51, H 5.26, N 6.74. $C_7H_{11}F_2NO_2Si$. Calculated, %: C 40.56, H 5.35, N 6.75. IR spectrum ($CHCl_3$, ν, cm^{-1}): 1730 m, 1660 s, 1520 w (NCO). NMR ^1H ($CDCl_3$, δ, ppm): 0.45 t (3H, MeSi, $^3J_{HF}$ 5.1 Hz), 2.75 br.m (4H, $H^{3,5}$), 2.03 m (2H, H^4), 2.83 br.s (2H, NCH_2Si). NMR ^{13}C ($CDCl_3$, δ, ppm): 0.82 t (MeSi, $^2J_{CF}$ 21.6 Hz), 31.19 s ($C^{3,5}$), 16.65 s (C^4), 27.52 t (NCH_2, $^2J_{CF}$ 26.8 Hz), 173.82 s (C=O). NMR ^{19}F ($CDCl_3$, δ, ppm): –130.45. NMR ^{29}Si ($CDCl_3$, δ, ppm): –30.22 t ($^1J_{SiF}$ 253.4 Hz).

Acknowledgment

This work supported by the Russian Foundation for Basic Research (grants Nos 16-03-00957 and 16-03-00984).

References

1. D. Kost, I. Kalikhman, in The Chemistry of Organic Silicon Compounds, ed. Z. Rappoport and Y. Apeloig, J. Willey, Chichester, 1998, vol. 2 (Part 1), pp. 1339–1445.
2. M.G. Voronkov, V.A. Pestunovich, Yu.I. Baukov, Organomet. Chem. USSR, 4 (1991) 593.
3. C. Chuit, R.J.P. Corriu, C. Reyé, J.C. Young, Chem. Rev., 93 (1993) 1371.
4. V.V. Negrebetsky, Yu.I. Baukov, Russ. Chem. Bull. (Int. Ed.), 46 (1997) 1807.
5. V.V. Negrebetsky, S.N. Tandura, Yu.I. Baukov, Russ. Chem. Rev., 78 (2009) 21.
6. A.A. Nikolin, V.V. Negrebetsky, Russ. Chem. Rev., 83 (2014) 848.
7. M.N. Sohail, R. Panish, A. Bowden, A.R. Bassindale, P.G. Taylor, A.A. Korlyukov, D.E. Arkhipov, L. Male, S. Callear, S.J. Coles, M.D. Hursthouse, R.W. Harrington, W. Clegg, Dalton Trans., 42 (2013) 10971.
8. S. Muhammad, A.R. Bassindale, P.G. Taylor, L. Male, S.J. Coles, M.B. Hursthousw, Organomet., 30 (2011) 564.
9. A.A. Nikolin, E.P. Kramarova, A.G. Shipov, Yu.I. Baukov, V.V. Negrebetsky, A.A. Korlyukov, D.E. Arkhipov, A. Bowden, S.Yu. Bylikin, A.R. Bassindale, P.G. Taylor. Organometallics, 31 (2012) 4988.
10. A.A. Nikolin, E.P. Kramarova, A.G. Shipov, Yu.I. Baukov, V.V. Negrebetsky, D.E. Arkhipov, A.A. Korlyukov, A.A. Lagunin, S.Yu. Bylikin, A.R. Bassindale, P.G. Taylor, RSC Advances, 6 (2016) 75315.
11. C.H. Yoder, C.M. Ryan, G.F. Martin, P.S. Ho, J. Organometal. Chem., 190 (1980) 1.
12. V.A. Pestunovich, S.V. Kirpichenko, N.F. Lazareva, A.I. Albanov, M.G. Voronkov, J. Organomet. Chem., 692 (2007) 2160.
13. E.P. Kramarova, A.G. Shipov, Vad.V. Negrebetsky, Yu.I. Baukov, Zh. Obshch. Khim., 67 (1997) 1403.
14. A.G. Shipov, E.P. Kramarova, O.B. Artamkina, Yu.E. Ovchinnikov, Yu.I. Baukov, Zh.

Obshch. Khim., 67 (1997) 1680.

15. A.G. Shipov, E.P. Kramarova, S.A. Pogozhikh, Vad.V. Negrebetsky, L.S. Smirnova, O.B. Artamkina, S.Yu. Bylikin, Yu.E. Ovchinnikov, Yu.I. Baukov, Russ. Chem. Bull., Int. Ed., 56 (2007) 461.
16. E.A. Zelbst, Yu.E. Ovchinnikov, A.A. Kashaev, N.F. Lazareva, V.P. Baryshok, Yu.T. Struchkov, M.G. Voronkov, Dokl. Chem. USSR, 327 (1992) 336.
17. V.V. Negrebetsky, P.G. Taylor, E.P. Kramarova, A.G. Shipov, S.A. Pogozhikh, Y.E. Ovchinnikov, A.A. Korlyukov, A. Bowden, A.R. Bassindale, Y.I. Baukov, J. Organomet. Chem., 693 (2008) 1309.
18. M.G. Voronkov, E.A. Zelbst, V.S. Fundamenskii, A.A. Kashaev, L.I. Gubanova, N.N. Chipanina, Yu.L. Frolov, Dokl. Chem. USSR, 292 (1987) 859.
19. G. Binsch, in Dynamic Nuclear Magnetic Resonance Spectroscopy, ed. L.M. Jackman, F.A. Cotton and R.D. Adams, Academic Press, New York, 1975, p. 45.
20. Vad.V. Negrebetsky, P.G. Taylor, E.P. Kramarova, S.Yu. Bylikin, I.Yu. Belavin, A.G. Shipov, A.R. Bassindale, Yu.I. Baukov, J. Organometal. Chem., 691 (2006) 3976.
21. Yu.I. Baukov, Yu.E. Ovchinnikov, A.G. Shipov, E.P. Kramarova, Vad.V. Negrebetsky, Yu.T. Struchkov, J. Organometal. Chem., 536–537 (1997) 399.
22. I. Ugi, D. Marquarding, H. Klusacek, G.W. Gokel, P. Gillespie, *Angew. Chem.*, 82 (1970) 703.
23. I. Ugi, I. Marquarding, H. Klusacek, P. Gillespie, Acc. Chem. Res., 4 (1971) 288.
24. A.L. van Geet, Analyt. Chem., 42 (1970) 679.
25. G. Haegele, R. Fuhler, Th. Lenzen, Comp. Chem., 19 (1995) 277.
26. G.M. Sheldrick, Acta Cryst., A64 (2008) 112.
27. G.M. Sheldrick, Acta Cryst., C71 (2015) 3.
28. O.V. Dolomanov, L.J. Bourhis, R.J. Gildea, J.A.K. Howard, H. Puschmann, *J. Appl. Cryst.* 42 (2009) 339.
29. M.J. Frisch, G.W. Trucks, H.B. Schlegel, G.E. Scuseria, M.A. Robb, J.R. Cheeseman, J. Montgomery, T. Vreven, K.N. Kudin, J.C. Burant, J.M. Millam, S.S. Iyengar, J. Tomasi, V. Barone, B. Mennucci, M. Cossi, G. Scalmani, N. Rega, G.A. Petersson, H. Nakatsuji, M. Hada, M. Ehara, K. Toyota, R. Fukuda, J. Hasegawa, M. Ishida, T. Nakajima, Y. Honda, O. Kitao, H. Nakai, M. Klene, X. Li, J.E. Knox, H.P. Hratchian, J.B. Cross, V. Bakken, C. Adamo, J. Jaramillo, R. Gomperts, R.E. Stratmann, O. Yazyev, A.J. Austin, R. Cammi, C. Pomelli, J.W. Ochterski, P.Y. Ayala, K. Morokuma, G.A. Voth, P. Salvador, J.J. Dannenberg, V.G. Zakrzewski, S. Dapprich, A.D. Daniels, M.C. Strain, O. Farkas, D.K. Malick, A.D. Rabuck, K. Raghavachari, J.B. Foresman, J.V. Ortiz, Q. Cui, A.G. Baboul, S. Clifford, J. Cioslowski, B.B. Stefanov, G. Liu, A. Liashenko, P. Piskorz, I. Komaromi, R.L. Martin, D.J. Fox, T. Keith, Al-

M.A. Laham, C.Y. Peng, A. Nanayakkara, M. Challacombe, P.M.W. Gill, B. Johnson, W. Chen, M.W. Wong, C. Gonzalez, J.A. Pople, Gaussian 03, C.01.

30. G.A. Zhurko, D.A. Zhurko, 2011, Chemcraft Program, Academic version 1.7
31. A.E. Pierce. Silylation of Organic Compounds: A Technique for Gasphase Analysis. Pierce Chemical Co., Rockford III, Illinois. 1968, 487 pp.

Supporting materials

Table 1s. Principal bond length and angles in isomers of compounds **1c**, **2a**, **2b** and **3** calculated by PBE0/6-311G(d,p) method/basis combinations

	Si1–F1	Si1–F2	Si1–O1	Si1–C1	F1–Si1–O1
1c-*c*	1.652/1.671	1.622/1.636	2.146/2.049	1.858/1.860	172.17/172.69
1c-*a*	n.a.	n.a.	n.a.	n.a.	n.a.
1c-*mea*	1.625/1.634	1.621/1.634	2.192/2.114	1.876/1.881	178.97/179.90
2a-*c*	1.653/1.672	1.621/1.635	2.138/2.044	1.858/1.861	172.11/172.80
2a-*a*	1.619/1.623	1.616/1.620	3.538/3.652	1.840/1.839	117.59/129.47
2a-*mea*	1.622/1.635	1.622/1.635	2.179/2.096	1.878/1.883	179.27/179.97
2c-*c*	1.656/1.674	1.622/1.635	2.089/2.012	1.858/1.860	171.44/172.26
2c-*a*	n.a./1.622	n.a./1.615	n.a./3.598	n.a./1.838	n.a./149.00
2c-*mea*	1.623/1.636	1.623/1.636	2.116/2.047	1.880/1.884	178.68/179.64
3-*c*	1.637/ 1.653	1.615/ 1.627	2.340/ 2.207	1.851/ 1.853	171.93/ 172.4
3-*a*	n.a./1.615	n.a./1.617	n.a./3.093	n.a./1.842	n.a./172.67
3-*mea*	n.a./1.619	n.a./1.620	n.a./2.439	n.a./1.859	n.a./179.21

a – acyclic isomer

c – cyclic isomer (most stable)

mea – isomer with a methyl group in apical position

n.a. – not available

Scheme 1

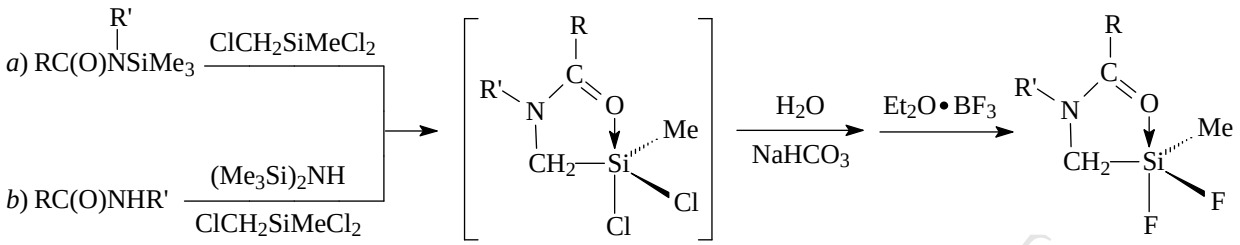

A **1a–c**

R = Ph, R' = H (**1a**); R = R' = Me (**1b**); R = Me, R' = CH(Ph)Me (**1c**)

Chart 1

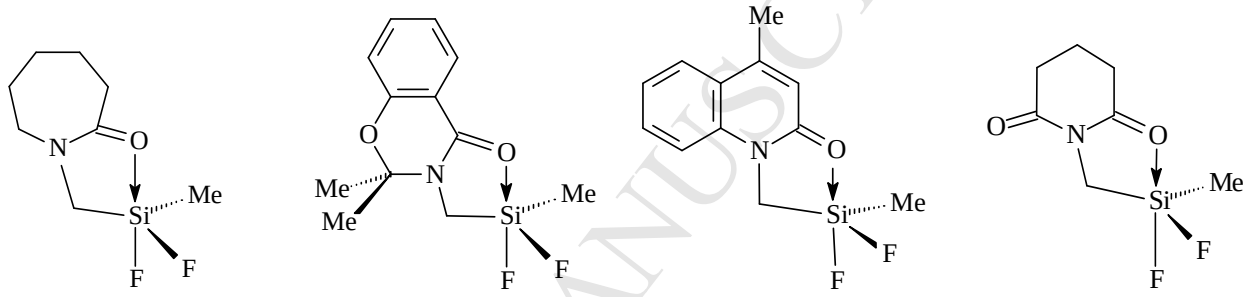

2a **2b** **2c** **3**

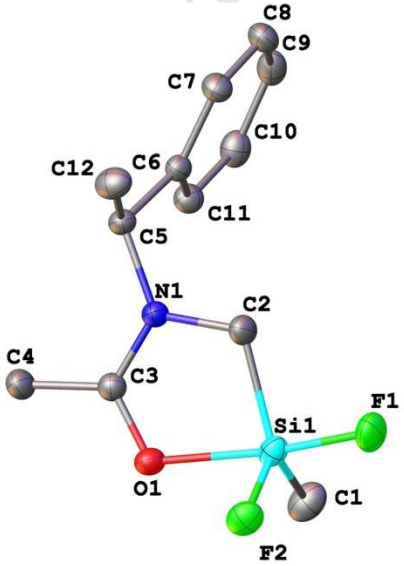

Figure 1. Molecular structure of **1c** in ADP ellipsoids at 50% probability.

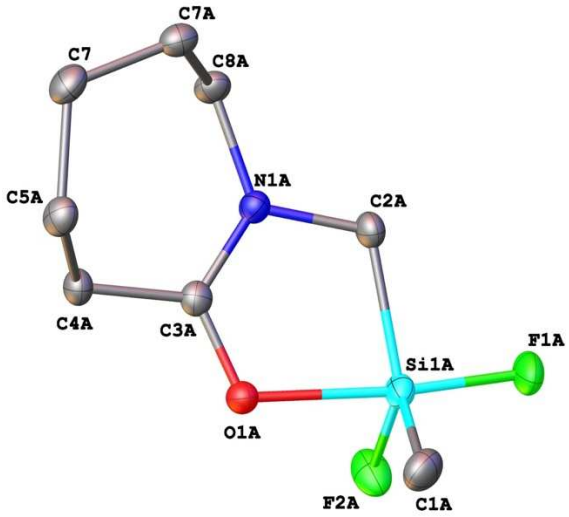

Figure 2. Molecular structure of **2a** in ADP ellipsoids at 50% probability.

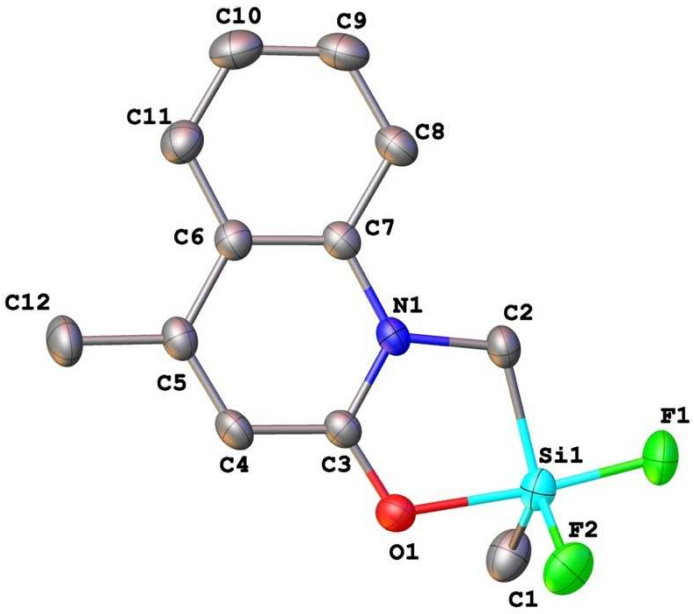

Figure 3. Molecular structure of **2c** in ADP ellipsoids at 50% probability.

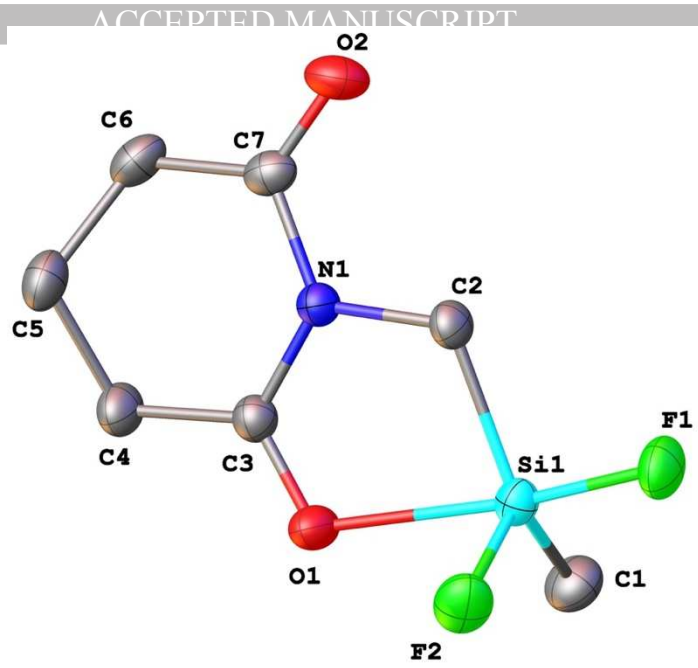

Figure 4. Molecular structure of **3** in ADP ellipsoids at 50% probability.

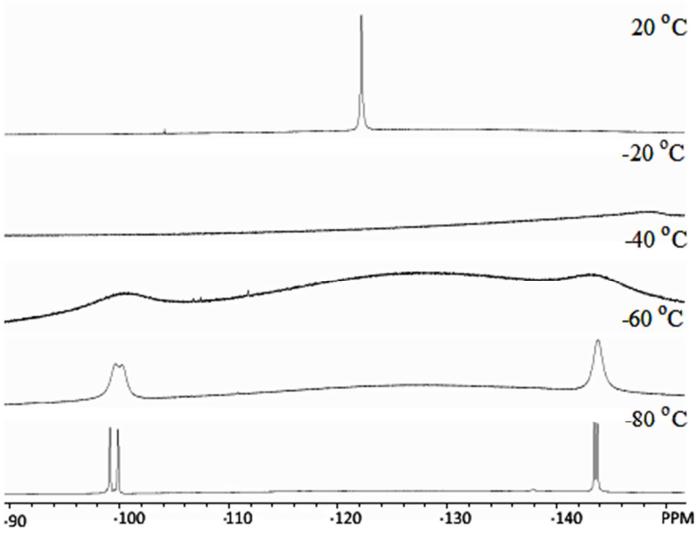

Figure 5. DNMR ^{19}F spectra of difluoride **1c** (Jeol JNM-EX400, CD_2Cl_2 + $CDCl_3$).

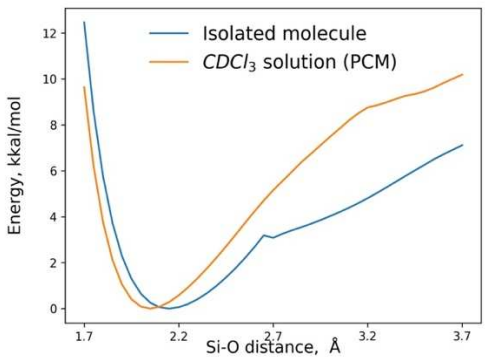

(a)

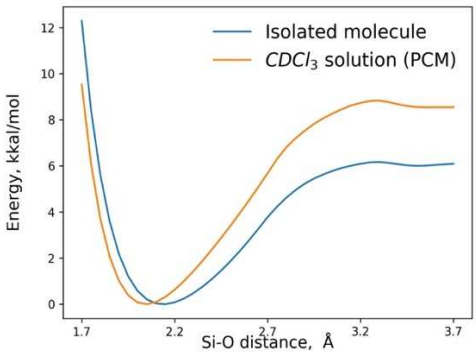

(b)

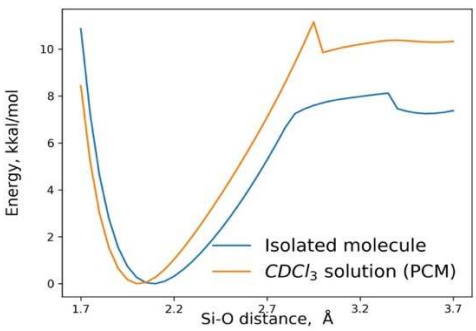

(c)

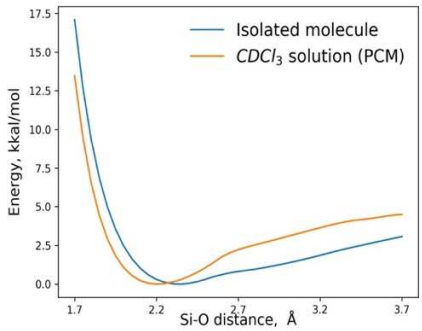

(d)

Figure 6. Relaxed energy scan using the O→Si coordination bond as the coordinate for **1c** (a), **2a** (b), **2c** (c), and **3** (d).

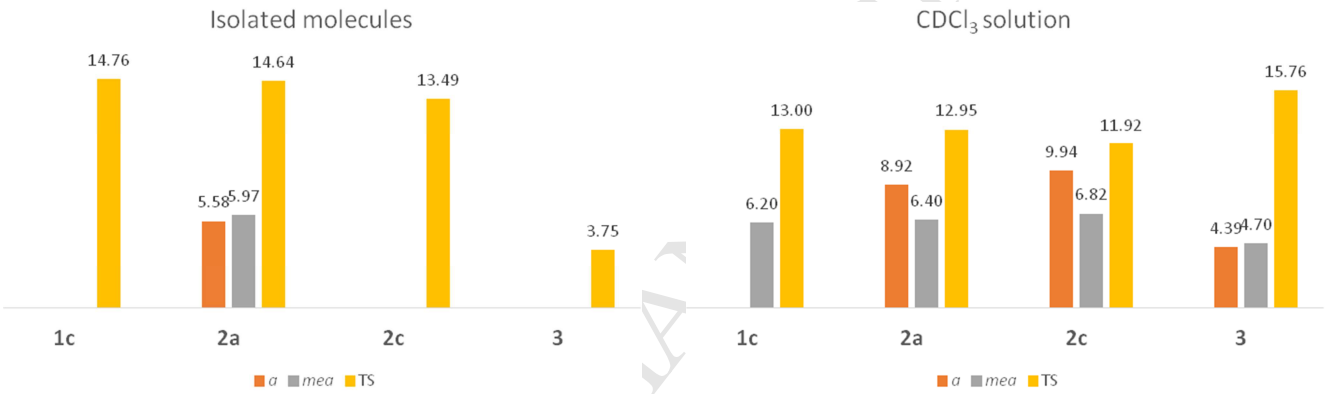

Figure 7. The energies (kcal mol^{-1}) of stationary points and transition states found on the PES of molecules **1c**, **2a**, **2c** and **3** in the gas phase (left) and in $CDCl_3$ solution (right). All values are relative to the most stable cyclic isomer.

Scheme 2